The influence of large landslides on river incision in a transient landscape: Eastern margin of the Tibetan Plateau (Sichuan, China)

William B. Ouimet†
Department of Earth, Atmospheric, and Planetary Sciences, Massachusetts Institute of Technology, Cambridge, Massachusetts 02139, USA

Kelin X. Whipple
School of Earth and Space Exploration, Arizona State University, Tempe, Arizona 85287, USA

Leigh H. Royden
Department of Earth, Atmospheric, and Planetary Sciences, Massachusetts Institute of Technology, Cambridge, Massachusetts 02139, USA

Zhiming Sun
Zhiliang Chen
Chengdu Institute of Geology and Mineral Resources, Chengdu, Sichuan Province, China

ABSTRACT

Deep landscape dissection by the Dadu and Yalong rivers on the eastern margin of the Tibetan plateau has produced high-relief, narrow river gorges and threshold hillslopes that frequently experience large landslides. Large landslides inundate river valleys and overwhelm channels with large volumes (>10^5 m^3) of coarse material, commonly forming stable landslide dams that trigger extensive and prolonged aggradation upstream. These observations suggest that strong feedbacks among hillslope processes, channel morphology, and incision rate are prevalent throughout this landscape and are likely characteristic of transient landscapes experiencing large increases in local relief, in general. Landslide effects are a by-product of rapid incision initiated by regional uplift. However, over timescales relevant to landscape evolution (>10^4 yr), large landslides can also act as a primary control on channel morphology and longitudinal river profiles, inhibiting incision and further preventing the complete adjustment of rivers to regional tectonic, climatic, and lithologic forcing.

We explore a probabilistic, numerical model to provide a quantitative framework for evaluating how landslides influence bedrock river incision and landscape evolution. The time-average number of landslide dams along a river course, and thus the magnitude of the landslide influence, is set by two fundamental timescales—the time it takes to erode landslide deposits and erase individual dams and the recurrence interval of large landslides that lead to stable dams. Stable, gradually eroding landslide dams create mixed bedrock-alluvial channels with spatial and temporal variations in incision, ultimately slowing long-term rates of river incision, thereby reducing the total amount of incision occurring over a given length of river. A stronger landslide effect implies that a higher percentage of channel length is buried by landslide-related sediment, leading to reduced river incision efficiency. The longer it takes a river channel to incise into a landslide dam and remove all landslide-related sediment, the more control these events have on the evolution of the river profile and landslide evolution. This can be the result of slow erosion of stable dams, or a higher frequency of large events.

Keywords: Asia, Tibetan plateau, geomorphology, river incision, landslides, transient rivers, landscape evolution, Dadu River

INTRODUCTION

Landslides are an important erosional process in all landscapes with moderate to steep hillslopes. In rapidly uplifting and incising fluvial landscapes, where high-relief, threshold hillslopes, and relatively narrow river gorges are common, landslides dominate hillslope erosion (Schmidt and Montgomery, 1995; Burbank et al., 1996), and large landslides often fill river valleys, forming landslide dams that inundate upstream channels with water and sediment (Costa and Schuster, 1988). The formation and failure of dams resulting from large mass wasting events such as catastrophic landslides, rockfalls, and rock avalanches are well-documented and have been studied extensively around the world (Costa and Schuster, 1991). Landslide dam stability and the style of dam failure (i.e., catastrophic or gradual) depend on the size and geometry of the blockage and material characteristics such as texture and sorting. Not all landslide dams fail quickly and/or catastrophically; many stabilize and block river valleys for hundreds to tens of thousands of years, with significant consequences for river morphology.

In this paper, we explore the influence of large landslides and landslide dams in the context of bedrock river incision and landscape evolution. Recent studies on this topic have emphasized the enduring influence of large, catastrophic landslides on deposition and erosion in the Indus River within the northwest Himalaya (Hewitt, 1998; 2006), and the effects of large landslides and landslide dams on the channel morphology and longitudinal profiles of rivers in southwest New Zealand, the Swiss Alps, Tien Shan, and the Himalayas (Korup, 2005; 2006; Korup et al., 2006). Both of these authors point out that landslide effects are superimposed onto the other controls of river profile and landscape evolution,

†wouimet@mit.edu

GSA Bulletin; November/December 2007; v. 119; no. 11/12; p. 1462–1476; doi: 10.1130/B26136.1; 10 figures; 1 table; Data Repository item 2007216.

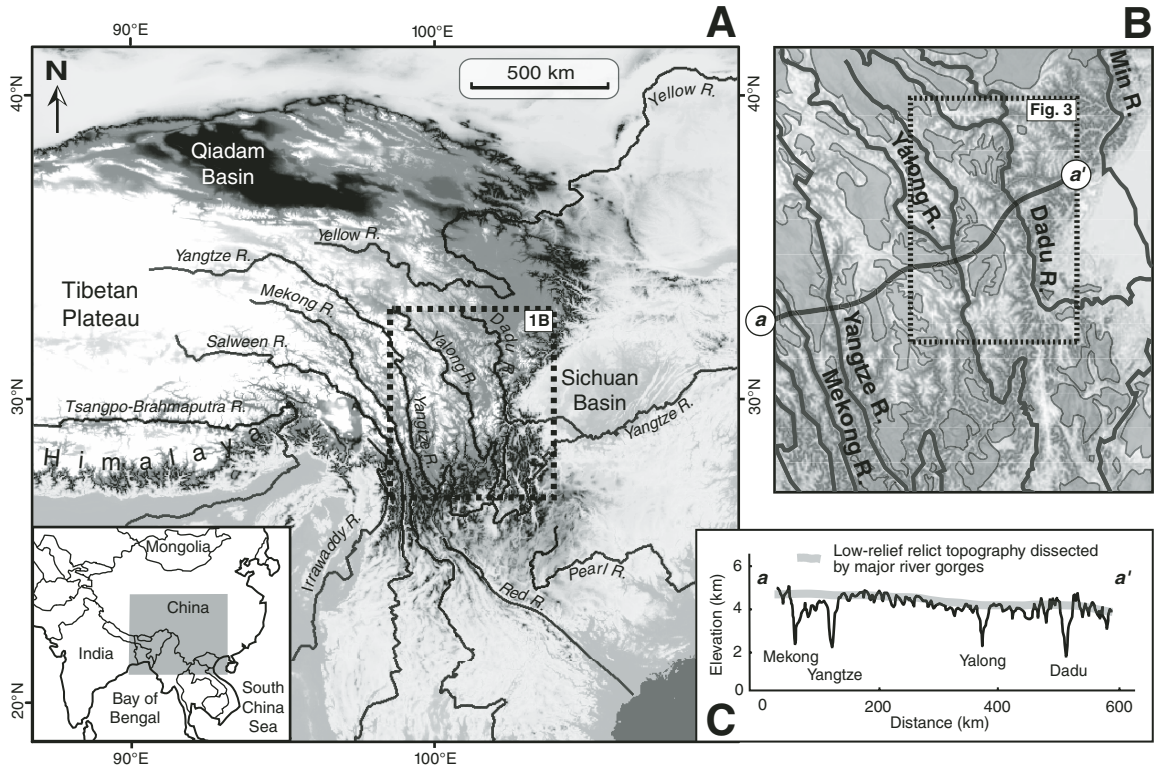

Figure 1. (A) Regional topography and rivers of the eastern margin of the Tibetan Plateau, a transient landscape characterized by deep river gorges cut into an uplifted, low-relief relict landscape. (B) Patches of low-relief, relict landscape preserved at high elevations. For a detailed description of the criterion used to identify patches of relict landscape, see Clark et al., 2006. (C) Topographic cross-section (path *a* to *a′* indicated in B), extracted from the ~1-km resolution GTOPO30 Digital Elevation Model (U.S. Geological Survey, 1993).

such as tectonics, climate, lithology, and base-level fall, and that a better understanding of the influence of landslides is needed before valley landforms and channel morphology can be used to infer the effects of these external forcings.

Deep landscape dissection on the eastern margin of the Tibetan Plateau has produced high-relief, narrow river gorges and threshold hillslopes that frequently experience large landslides, making the entire region highly susceptible to landslide dams. Here, we use key examples from the Dadu and Yalong river gorges (Fig. 1) to highlight the influence of large landslides and the interaction between landslide dams, channel morphology, longitudinal river profiles, and river incision. We then develop a numerical model to simulate the occurrence and erosion of landslide dams along a length of river, and examine long-term controls on the degree to which channels may be buried by landslide-related sediment and inhibit river incision. Our model is an important step toward quantifying the influence of large landslides in actively incising landscapes and incorporating this influence into models of bedrock river incision and landscape evolution.

Overview of Stable Landslide Dam Formation and Effects on Rivers

A stable landslide dam is any landslide dam that stabilizes and blocks a river valley for hundreds to tens of thousands of years, either initially or after some degree of catastrophic failure and dam-outburst flood erosion. Landslide deposits that fill river valleys and consist of a high percentage of large (>2 m) boulders or deflect rivers over bedrock ridges often lead to the formation of stable landslide dams. Once upstream lake levels reach the top of the landslide dam and streamflow over landslide deposits begins, erosion-resistant boulders armor the channel bed as finer material is washed downstream. This process condenses the original landslide material to a smaller mass composed of large boulders, stabilizing the landslide dam, and protecting the top of the initial deposit from further erosion. These large boulders are not easily moved in even large floods, and serve to roughen the bottom of the channel. There is often evidence of advanced fluvial sculpting of boulders, which attests to long periods of boulder stability. In these steep reaches, dramatic rapids form and river channels narrow. Upstream of landslide dams, river gradients are low, and fine-grained lake sediments and alluvial gravels accumulate. In conjunction with filling within the trunk river, side tributaries may become filled with alluvial fans graded to the high fill level of the trunk stream. The abrupt change in slope associated with the transition from upstream, low-gradient fills to steep, dramatic rapids through the landslide deposits creates significant knickpoints with a drop in elevation of up to 100- to 300-m (Korup, 2006).

The integrated effects of large landslides on river channels completely prohibit rivers from eroding their bed and incising over the length of the landslide mass and associated fill deposits. This period of local non-incision continues for the entire duration of a landslide dam event, from the emplacement of the dam, to complete incision through landslide deposits and some portion of the associated upstream fill. During this time, the long-term evolution of the river profiles and landscape evolution are affected in two main ways: (1) downstream reaches continue to incise, while landslide reaches do not, and (2) filled upstream reaches and the whole profile upstream

of the fill effectively have a new, unchanging base level that freezes all further adjustment (i.e., upstream migration of downstream incision signals). Therefore, within actively incising landscapes, large landslides establish spatial and temporal variations in incision rate, even if rock uplift is steady and uniform.

Whether or not large landslides have significant long-term effects on river incision depends on the longevity of individual landslide dams and their distribution in space and time. Landslide occurrence and distribution depends on material properties, landslide triggers (i.e., heavy precipitation and earthquakes), and the degree to which hillslopes are over-steepened and primed for massive failure. Longevity of individual landslide dams is a function of dam geotechnical stability and river incision into the landslide deposit. The stability of landslide dams depends on a number of factors, most important of which are the size of the original landslide deposit, the percentage of large boulders within that deposit, and the geometry of the valley filled (Costa and Schuster, 1988). The percentage of boulders within the landslide deposit is a function of bedrock strength, landslide process, and depth of failure. Local bedrock lithology is important here because it controls the cohesive strength of hillslope material and determines the size of the material within the landslide deposits, largely as a function of how massive, fractured, or layered is the bedrock in the area.

The geometry of river valleys affects whether or not stable landslide dams form and change in response to large hillslope failures. Rapid deposition of landslide debris deflects river channels within their valleys, and subsequent incision into landslide debris and upstream fill deposits may involve bedrock ridges of the former valley, enhancing the stability and duration of the landslide blockage. Narrow, bedrock-walled valleys constrict landslide deposits and force rivers to incise directly into landslide deposits, limiting lateral mobility in the valley. Narrow valleys are also, in general, more likely to concentrate large landslide deposits in the channel, leading to stable dams. Big rivers characteristically have wide valleys, therefore requiring bigger landslides, if stable landslide dams are to form. Large landslides change the geometry of river valleys by widening the valley floor and reducing hillslope relief, which can drive the lateral erosion of hillslopes and redefine drainage divides, such as has been recognized in physical experiments of landscape evolution (Hasbargen and Paola, 2000). Most landscape evolution models do not realistically treat large landslides. This omission may, in part, explain the far greater stability of river networks in numerical simulations of landscape evolution.

Landslides, Bedrock River Incision, and Landscape Evolution

The persistence of landslide dams within actively incising river gorges such as those on the eastern margin of the Tibetan Plateau is one aspect of the dynamic coupling between bedrock river incision and hillslope erosion that can significantly influence the evolution of fluvial landscapes. Hillslopes occupy a much higher percentage of landscape area, therefore accounting for most of the denudation that occurs, but bedrock river incision generates local relief and ultimately controls regional erosion rates by setting the boundary condition for hillslope erosion to occur (e.g., Whipple, 2004). However, to incise, rivers must both erode bedrock and transport all the sediment supplied to them from the entire upstream drainage basin and adjacent hillslopes (e.g., Sklar and Dietrich, 1998). This suggests that an important negative feedback may exist within rapidly incising landscapes, where hillslope erosion, following incision, slows and/or stops river incision by covering the bed for an extended period of time with larger volumes of material or coarser grain sizes of sediment than annual floods can easily transport downstream. Aspects of this feedback are contained in sediment flux–dependent river incision models that emphasize the dual role of sediment as both a tool for erosion and an element inhibiting erosion by covering the channel bed (Sklar and Dietrich, 1998, 2001; Whipple and Tucker, 2002).

Large landslides can influence river profiles over timescales relevant to landscape evolution (>10^4 yr), and as a result, there is a need to develop models that incorporate their effects on bedrock river incision and landscape evolution (Hewitt, 1998; Korup, 2002). Localized, large, hillslope-sediment input is seldom incorporated into models and dynamics of long-term, longitudinal river profiles and landscape evolution. The landslide effect described here acts over and above the more continuous sediment supply effects considered in recent modeling studies (e.g., Sklar and Dietrich, 2004, 2006; Gasparini et al., 2006). Many models of hillslope evolution have no expression for landslide erosion on hillslopes (e.g., Tucker et al., 2001). Densmore et al. (1998) provide the most detailed landscape evolution model in terms of landslide erosion, emphasizing the full range of landslide erosion and the role of large landslides, but their approach does not allow for a dynamic coupling between bedrock river incision and hillslope erosion. Instead, all material that landslides deliver to the channel in their model is regolith and transportable by fluvial processes, and significant channel blockages with lakes and upstream sedimentation do not occur (Densmore et al., 1998).

The influence of large landslides is another way bedrock river incision and landscape evolution may be affected by tectonics and/or climate, which can vary across space and time throughout a landscape. There are clear, well-documented relationships between earthquake size and the probability of large landslides (Keefer, 1994). In addition, changes in the intensity of precipitation, such as increases in the monsoonal precipitation on the Himalaya, have been directly linked with increases in the occurrence of large landslides, and subsequent periods of fluvial aggradation (Pratt et al., 2002; Trauth et al., 2003; Bookhagen et al., 2005). Tectonics also influences the frequency and potential magnitude of landslide events more generally through increases in topographic relief and erosion rates driven by rock uplift.

By influencing river incision, landslides affect the form of river profiles and can significantly complicate their interpretation (Korup, 2006). The shape and the slope-area relationships of river profiles have been used by many researchers to infer patterns of rock uplift (Kirby et al., 2003; Lague et al., 2003; Kobor and Roering, 2004; Wobus et al., 2006). However, there is a strong link between profile knickpoints, channel steepness, and the occurrence of large landslides. Some of the steepest channels and highest channel-steepness index values anywhere within a landscape may be associated with channel steepening through landslides (Korup, 2006). River profiles are also used to study the characteristics of transient landscapes (Gasparini, 2003; Crosby and Whipple, 2006; Gasparini et al., 2006; Wobus et al., 2006). Two end-member models of bedrock river incision are detachment-limited models (where incision is regulated by the detachment and abrasion of the bedrock channel bed) or transport-limited models (where incision is regulated by transport of sediment) (Willgoose et al., 1991; Howard, 1994; Whipple and Tucker, 2002). These models predict different forms for transient river profiles. However, landslide effects may lead to the same transient morphologies as bedrock river profiles evolving under detachment- and transport-limited conditions—abrupt knickpoints as in detachment-limited models and smooth, diffuse, convexities as in transport-limited models. The two case studies we discuss in the next section are examples of both these situations.

STUDY AREA

The eastern margin of the Tibetan Plateau is one of the world's broadest and most dramatic transient landscapes, characterized by a regionally persistent, elevated, low-relief relict landscape that has been deeply dissected by major

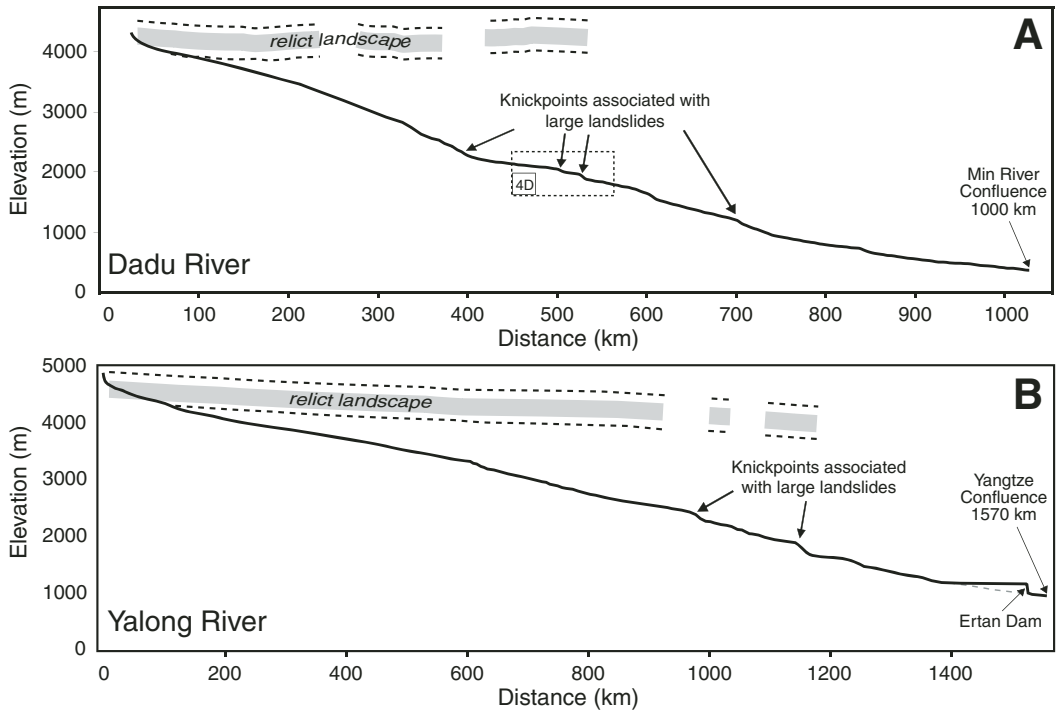

Figure 2. Longitudinal river profiles of the Dadu River (A) and Yalong River (B), extracted from ~90-m resolution Shuttle Radar Topography Mission (SRTM) data. In areas where SRTM data are missing within the river gorge, the profile is inferred from adjacent points. Solid-gray lines drawn above the profiles indicate where patches of relict landscape are well preserved within a distance of 20–30 km adjacent to the river gorges. Dashed lines indicate the relief bounds of the relict landscape (Clark et al., 2006). Each profile has a diffusive, smooth upper section rolling off the relict landscape, contrasted with a steep lower profile that has many knickpoints, some of which are associated with large landslides, as noted.

rivers and their tributaries (Clark et al., 2006; Fig. 1). Thermochronological data show that rates of rock cooling on the eastern margin of the plateau increased dramatically between 9 and 13 Ma, suggesting that uplift and major river incision began at that time (Kirby et al., 2002; Clark et al., 2005). Major rivers start at high elevations over 4000 m, where they are slightly incised into the relict landscape, and transition into rapidly incising, high-relief, dissected gorges with steep hillslopes (Fig. 2). Estimates of long-term (10^6–10^7 yr) bedrock river incision in these gorges are on the order of 0.25–0.5 mm/yr (Clark et al., 2005). Longitudinal river profiles exhibit transient morphologies, with large knickpoints, and convex to linear, rather than concave, profile forms. Hillslopes, following incision, display zones of adjustment with steepest values in the lowermost reaches of individual basins. These observations highlight the transient response of rivers to rapid incision on trunk streams as waves of landscape adjustment propagate upstream and up hillslopes.

The Dadu River (*Dadu He*) and Yalong River (*Yalong Jiang*) are major tributaries of the Yangtze River (*Jinsha Jiang*), both over 1000 km in length (Fig. 2). Bedrock geology in these catchments consists mainly of the Songpan-Ganze flysch terrane, which is intruded by a series of Jurassic age granitic plutons (Roger et al., 2004) and deformed Paleozoic rocks and crystalline Precambrian basement that outcrop in the southern portions of each catchment (Burchfiel et al., 1995). The most prominent active fault within these catchments is the Xianshuihe Fault, a large-scale, strike-slip fault slipping at ~10 mm/yr (~60 km total offset) that has experienced four earthquakes greater than magnitude 7 in the last century (Allen et al., 1991). The Dadu and Yalong rivers have each experienced catastrophic landslide damming events within the past 250 yr that were triggered by large, >6.0-M earthquakes (Tianchi, 1990; Dai et al., 2005). Accounts from the example on the Dadu River indicate as many as 100,000 deaths were caused by the downstream flooding associated with initial dam failure, making it one of the most disastrous events ever resulting from a landslide dam breach (Dai et al., 2005). Recent catastrophic events such as these have also been documented in the Min River gorge to the east of the Dadu and in the main Yangtze River gorge to the west of the Yalong, indicating that landslide damming is a widespread and ongoing phenomenon in all river gorges on the eastern margin (Tianchi, 1990; Hejun et al., 2000).

River Morphology and Large Landslides

Fieldwork conducted during 2003–2006 along the trunk streams and major tributaries of the Dadu and Yalong indicates that valleys contain a combination of fluvial and landslide deposits, tributary alluvial fans, lake sediments, debris-flow deposits, and bedrock (see Data Repository[1] for photos). Numerous low-gradient topographic benches 50–1000 m above the modern river level, previously interpreted as river terraces, were determined to be fluvially beveled landslide deposits, the tops of ancient landslide dams, or high levels of alluvial gravel and lake sediment associated with landslide deposits. Channel and valley widths vary greatly as channels alternate between straight, narrow-walled, steep, incising bedrock reaches and meandering, wide, gentle, depositional alluvial reaches. Bedrock reaches generally have steep bedrock hillslopes adjacent to channels. Hillslopes are also steep within alluvial reaches, but the large volume of sediment filling the valley in these reaches and the meandering nature of the channel disconnects channels from adjacent hillslopes and suggests that the bedrock valley floor is far below the present channel bottom.

Other than the occasional steep bedrock reaches, most steep reaches are boulder rapids, 10–1000 m long, that are found only in association with landslides, rockfalls, and debris flow deposits. Many of these rapids occur at the location of well-defined, large, deep-seated landslide events (>5×10^5 m^3) that are easily identified based on their morphology and textural characteristics (Fig. 3). These large landslides appear, in many cases, to have led to extensive and prolonged river damming, as deposits from large landslides frequently coincide with upstream sediment interpreted to be related to

[1]GSA Data Repository item 2007216, Figures DR1–DR7, is available at http://www.geosociety.org/pubs/ft2007.htm or by request to editing@geosociety.org.

impoundment and aggradation behind present and paleo-landslide dams (e.g., lake sediments and alluvial fill). Landslide deposits vary from large fragments of intact bedrock, variably brecciated and fractured, to a complete mix of unconsolidated, poorly sorted material ranging in size from pulverized rock, dust, and sand to 10- to 30-m-diameter boulders.

Depending on how recently the damming event occurred and how large the event was, river channels are incised into landslide deposits and upstream fill to varying degrees (Fig. 3). Some landslide dams still have lakes upstream, while others are completely filled in with alluvium upstream, with large alluvial fans graded to the height of the ancient landslide dam outlet level, some with picturesque villages built upon them indicating substantial antiquity. In other cases, preserved relics (lake sediments, alluvial fill, and ancestral tributary fans) of much older landslide dams high up on valley walls suggest extremely large damming events have occurred, or that damming events occurred when the trunk level was higher than it is today.

Throughout river gorges on the eastern margin of the Tibetan Plateau, we find a range of landslide dam sizes with stable heights between tens to hundreds of meters, affecting stretches of river ranging from hundreds of meters to over 20 km in length. The age of most of these landslide events is unknown; known ages range from modern examples (as recently as 1933) to ones reaching as far back as >40,000 yr (^{14}C age). We have dated three landslides with cosmogenic radionuclide (^{10}Be) exposure ages to ~8800, ~6500, and ~57,000 years old. We have also used optically stimulated luminescence (OSL) to date lake sediments associated with one ancient dam to ~5,000 yr old. In some cases, landslides linger within river gorges, influencing incision for 10^5–10^6 yrs (as indicated by at least one location where recurrent landslides and local rock properties appear to have effectively inhibited a major tributary from keeping pace with trunk-stream incision in the past ~9–13 m.y.). In some regions on the Dadu River, the integrated effect of many large landslides and dams appears to have effectively dammed stretches of river up to 100 km in length, forcing them to become alluviated.

Case Study 1: Dadu Gorge and Tributaries—Danba Region

The Danba region in the Dadu catchment hosts several excellent examples of the interaction between landslide dams, river profiles, and channel morphology (Fig. 4). The bedrock geology around Danba consists of a structural antiform that exposes deeper, deformed levels of the Paleozoic sequence beneath the Triassic-Jurassic Songpan-Ganze flysch, notably a

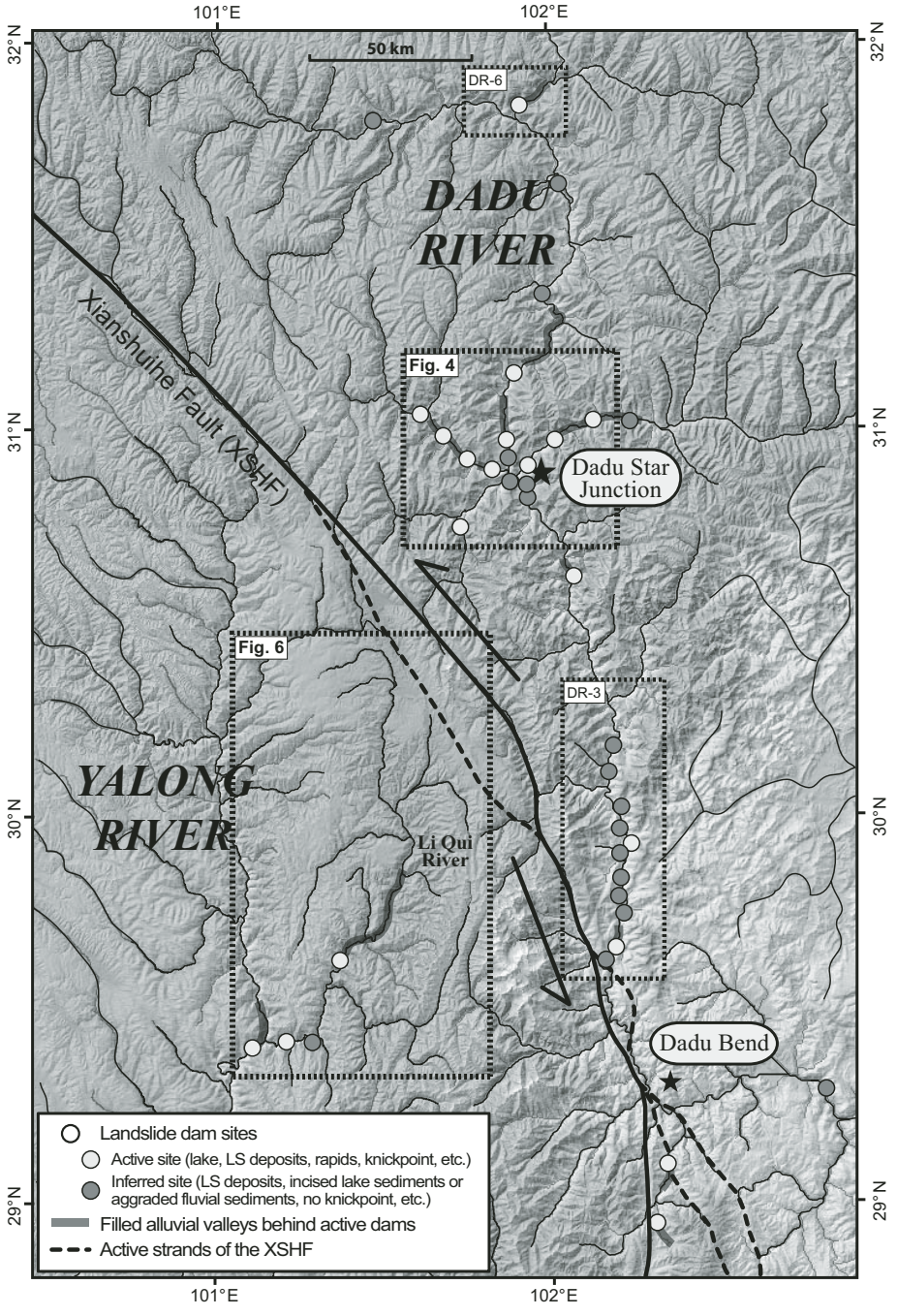

Figure 3. Landslide dam sites (active *and* inferred) within the Dadu and Yalong river gorges, superimposed on a shaded-relief rendering of the region. Identification based on morphology and characteristics of landslide deposits (typically >0.25 km^3) and landslide dam deposits (lake sediments, fill terraces, etc.). The main distinction between active and inferred sites is that active sites still define significant knickpoints on longitudinal profiles. Fieldwork was restricted to the Dadu River gorge, major tributaries near Danba, and the Li Qui River. Bold lines behind certain landslides indicate the degree to which river valleys are presently filled in with sediment behind large landslide dams. Note the location of Xianshuihe fault. Inset boxes refer to the locations of Figures 4, 6, DR-3, and DR-6. LS—landslides.

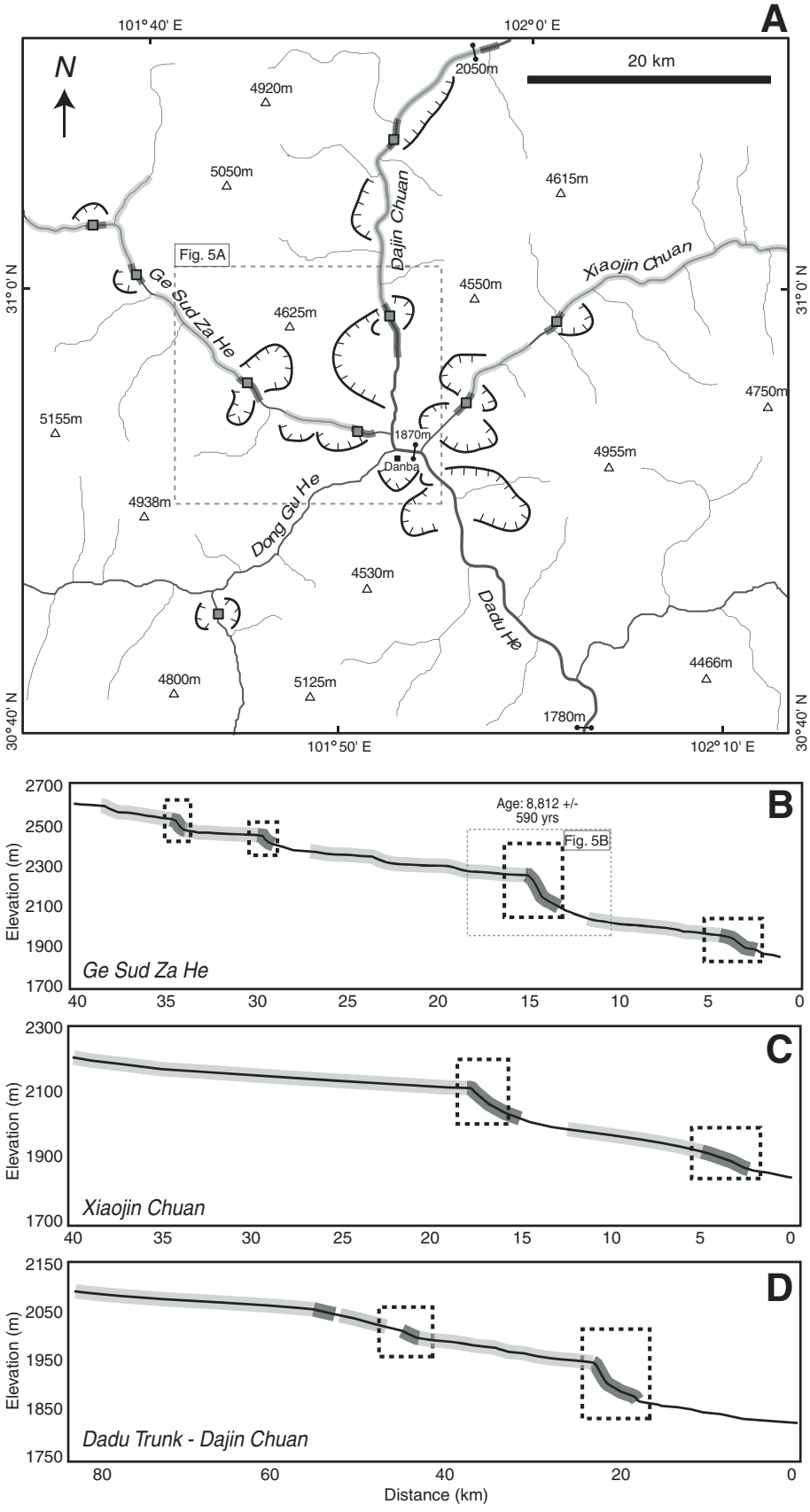

Figure 4. Danba region, Dadu River. (A) Map of the Danba region indicating the site of active landslide dams (gray boxes), landslide scars (bold black lines with teeth), landslide boulder rapids (dark-gray shading), and currently dammed/filled in stretches of river (light-gray shading). (B) Lower 40 km of the Ge Sud Za He River longitudinal profile, with four active landslide dams and associated upstream filling. (C) Lower 40 km of the Xiaojin Chuan River longitudinal profile, with two active landslide dams and associated upstream filling. (D) Longitudinal profile of the Dadu River through the Danba region, with two active landslide dams and associated upstream filling. Dashed boxes denote landslide deposits, scaled by estimated landslide volumes. All profiles extracted from ~90 m SRTM data. Inset boxes refer to location of Figures 5A and 5B. The ages of all landslide dams are unknown except for one noted.

Silurian mica-rich schist. This schist is prone to large landslides, and, consequently, hillslopes around Danba commonly have hummocky landslide morphology. At Danba, the Dadu trunk stream (named *Dajin Chuan* here) joins three large tributaries, the *Ge Sud Za He*, *Xiaojin Chuan*, and *Dong Gu He*, in a star-shaped pattern. Upstream from Danba, there are significant landslide-related knickpoints on the Dadu mainstem and on all three of these tributaries. The abrupt knickpoints in all these river profiles are related to landslides, with the same morphology as knickpoints created by rivers that cross a sharp lithologic contrast (i.e., weak rock type to strong), or by transient river response to upstream migration of incision in models of detachment-limited bedrock river incision (Whipple and Tucker, 2002).

The *Ge Sud Za He* tributary, in particular, is dominated by landslide dams, boulder rapids, and impounded alluvial fills for 40 km upstream of its confluence with the Dadu mainstem (Fig. 4). The most dramatic of these landslide dams occurs 15 km upstream from the confluence with the Dadu, with ~150 m of drop in the rapids caused by the landslide deposits. Field surveys show nicely the characteristic drop in channel width and increase in channel slope across the landslide mass where the channel is armored by large boulders (Fig. 5). This particular example shows a period of prolonged upstream filling, as numerous large alluvial fans upstream are graded into the new base level set by the landslide dam. The age of the landslide is 8,812 ± 590 yr, based

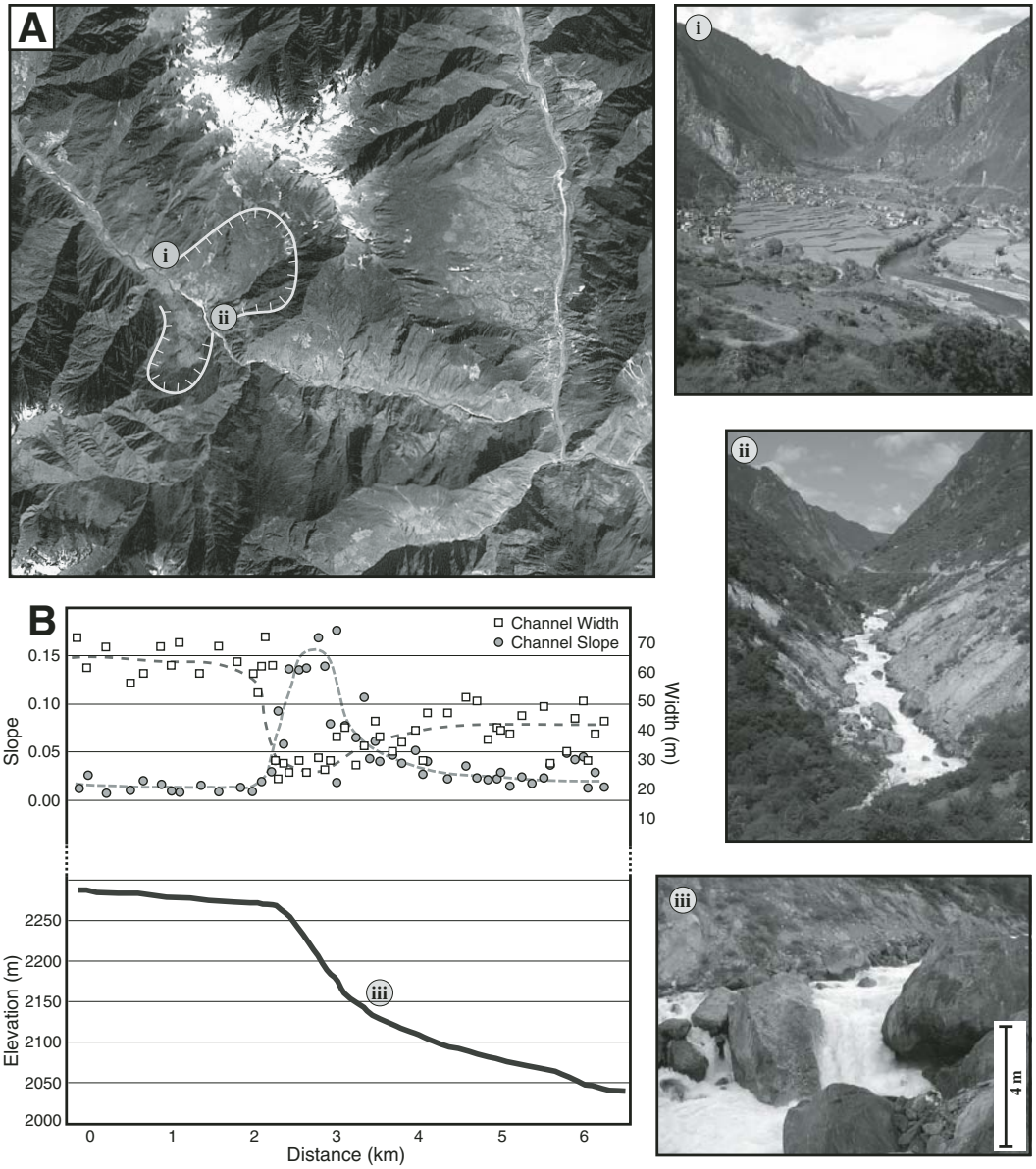

Figure 5. Ge Sud Za River landslide dam close-up, photos, and data. (A) LANDSAT satellite image, resolution 30 m; A-i and A-ii mark photo locations. (A-i) Field photo of the filled valley upstream with large alluvial fans adjusted to the present river level. (A-ii) Field photo of the steep narrow rapids through landslide deposits. (A-iii) Field photo of the steep, narrow rapids that are composed of large boulders of schist. (B) Profile, slope, and width data collected during a field survey; A-iii marks photo location. Note the drop in width and increase in channel slope at the top of the landslide dam.

on a cosmogenic radionuclide (^{10}Be) exposure age for a large, ~10-m-diameter boulder on top of the landslide deposit.

Case Study 2: Li Qui River

The Li Qui River is a 190-km-long tributary of the Yalong River, with 1800 m of fluvial relief, and a total drainage area of 5,880 km^2. The Li Qui drains off a low-relief landscape perched ~2–2.5 km above local base level and transitions into a rapidly incising, dissected landscape in its lower reaches, where a pronounced knickpoint on the longitudinal profile accounts for most (~1 km) of the fluvial relief (Fig. 6). Landslides have fundamentally altered the morphologic expression of the transient response of the Li Qui to mainstem incision on the Yalong. There is extensive evidence for the influence of landslides on valley and river profile geometry (Fig. 6D). Well-preserved lake and alluvial fill gravels record a period of prolonged river damming, but the river has subsequently incised into a portion of these sediments. The highest fill level increases in height moving downstream, and widespread landslide deposits indicate the likely site of an ancestral landslide dam. All fill levels end at the site of the inferred landslide dam ~40 km upstream of the Yalong confluence. Farther downstream, within the last 20 km before its confluence with the Yalong, the Li Qui River is extremely steep due to a combination of rapid base-level fall and large landslide debris within the present channel. This stretch of river is one of the steepest reaches of river in the Dadu and Yalong catchments, dropping at ~3.3% for 40 km, and it coincides with where the Li Qui River runs south of a granite intrusion. The large boulders seen in the channel along this stretch are granite, presumably delivered to the channel from rockfalls and landslides.

Barring the presence of an as-yet-unknown localized tectonic uplift, we surmise that the greater bed roughness created by these large, immobile unfractured boulders, together with their intrinsic resistance to abrasion, have significantly impeded the incision of the Li Qui River, leading to the formation of this ~1-km-high knickpoint. That channels are steeper crossing stronger, more erosion-resistant lithologies is to be expected, because rivers maintain steeper slopes and more erosive power to erode their bed

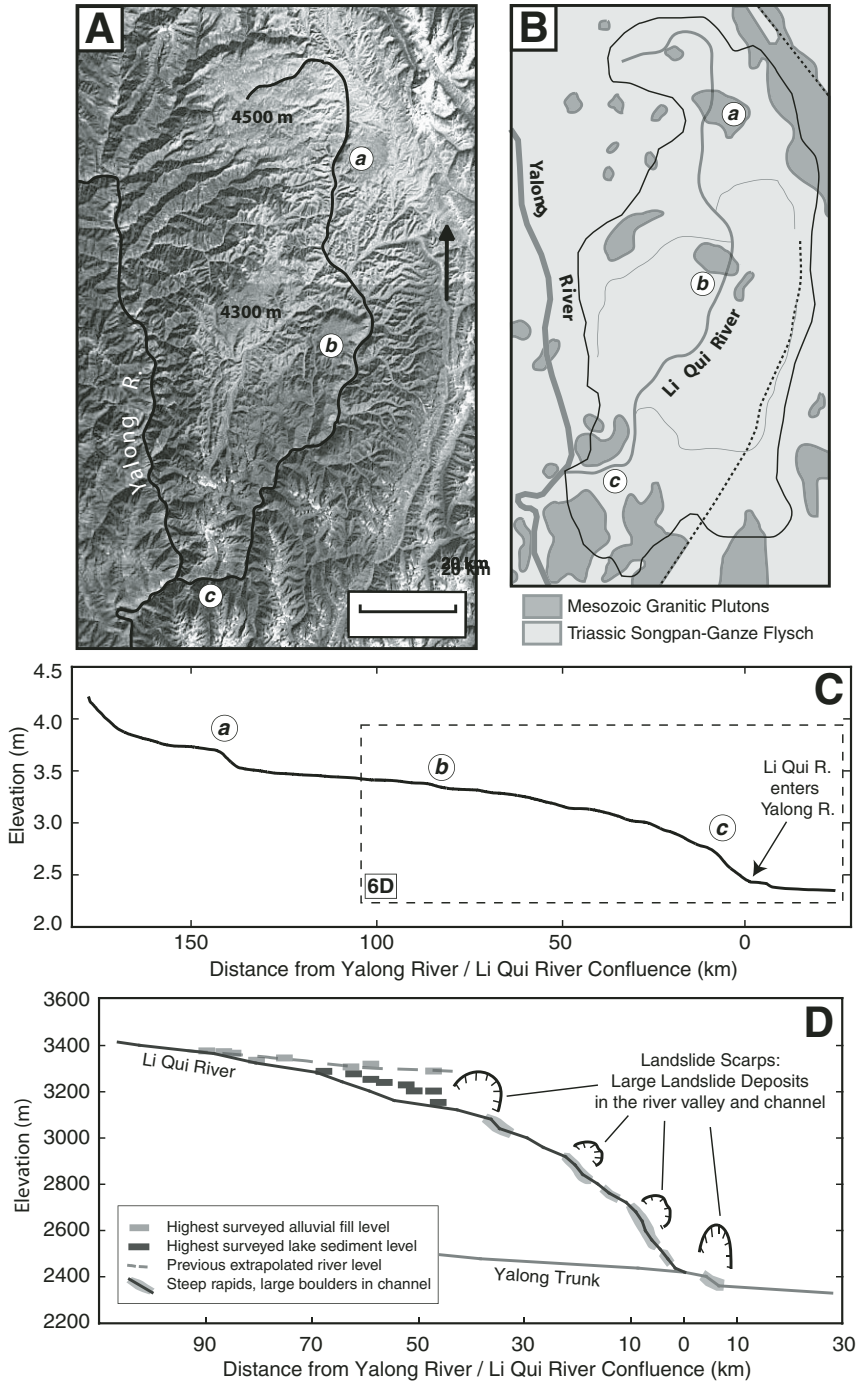

Figure 6. Li Qui River, tributary of Yalong River. (A) LANDSAT satellite image. (B) Simplified geologic map derived from "Geologic map of the Tibetan Plateau and adjacent areas," compiled by Chengdu Institute of Geology and Mineral Resources and Chinese Geological Survey (map scale 1:1,500,000). (C) Longitudinal river profile extracted from 90-m-resolution Shuttle Radar Topography Mission data. (D) Lower Li Qui River longitudinal river profile with mapping. Landslide damming and subsequent re-incision into the resulting fill deposit gives this profile its smooth, convex shape, accentuated by the effects of a strong, more resistant bedrock lithology (granite) outcropping in the region and the transient response to rapid incision on the Yalong River.

in these areas to keep pace with areas upstream and downstream. However, landslide effects suggest that channels are steeper at stronger, more erosion-resistant lithologies because it is harder to erode bedrock in those areas, and the massive nature of bedrock lithology in these areas yields large, erosion-resistant boulders during mass wasting events. The integrated effect of large landslides on the Li Qui is to prohibit bedrock incision and slow the upstream migration of incision on the Yalong trunk stream. This promotes the survival of large patches of relict landscape (see Figures 1 and 6A). Landslide damming and subsequent re-incision give the Li Qui longitudinal profile its smooth, convex shape, which otherwise might have been interpreted as representing a diffuse, transport-limited transient response to a base-level fall (e.g., Begin et al., 1980). Transient river profile form, therefore, is not simply diagnostic of alternate forms of bedrock river incision models as suggested by Whipple and Tucker (2002), but rather can reflect a complex combination of factors.

Numerical Modeling

The prevalence of landslide dams impacting river-channel morphology on the eastern margin of the Tibetan Plateau, and elsewhere (Korup et al., 2006), motivates us to formulate a quantitative framework for how landslides influence river incision, and, hence, landscapes in general. In this section, we develop a numerical model to simulate the occurrence and erosion of stable landslide dams along a length of river based on simple rules for the timing and magnitude of landslide events and generalized models for the erosion of individual dams once they stabilize. We also derive basic analytical expressions for the long-term average number of landslide dams along a river and relate them to the burial of bedrock valley floors and reduced river-incision efficiency.

Overview

The schematic in Figure 7A represents a snapshot in the evolution of rivers where landslide dams occur and erode through time, such as on the eastern margin. At any given time, there is a distribution of landslide dams along a length of river that may comprise all stages of erosional decay from fresh, uneroded dams to small remnants of previous dams. Each landslide dam is associated with a wedge of landslide deposits and aggraded material that buries bedrock valley floors and inhibits incision. The percentage of channel buried, which we call the landslide burial factor (*Bf*), is therefore a function of the number of landslide dams that exist and their heights above the bedrock floor (dam height

sets the upstream extent of aggraded alluvium; Fig. 7B). We can estimate *Bf* within river gorges on the eastern margin through a combination of field mapping and analysis of river profiles (Fig. 4; Table 1). These modern estimates of *Bf* are appropriate for, at most, the past 8000–10,000 yr, but we take them as being indicative of the long-term averages expected for these rivers. As we will show later in this section, *Bf* is roughly equivalent to the percentage of fluvial relief on rapids and falls associated with landslide knickpoints.

Our modeling is aimed at understanding what controls the average number and height of landslide dams along a river because these factors will directly, and significantly, affect the efficiency of river incision. These long-term averages imply an average sum of landslide dam heights and, therefore, a long-term average *Bf*. *Bf* is a direct measure of the influence of landslides on river-incision efficiency, since the fraction of the channel bottom not buried under deep fills, and thus generally available for incision (*Ba*) is 1-*Bf* (i.e., 0–1). Low values of *Ba* imply a stronger, more intense landslide effect with lower river-incision efficiency; values closer to one imply a weak, negligible landslide effect with river-incision efficiency close to what it should be in the absence of landslide dams. *Ba* can be considered a rough scaling factor that should modulate the coefficient of river incision (*K*) in many models. Analysis of the controls on *Ba* is thus a key to gauging the long-term, integrated influence of recurrent stable landslide dams. Our approach is to investigate the two fundamental timescales that together govern the long-term average number and heights of stable landslide dams, and, therefore, *Bf* and *Ba*. These are the landslide recurrence interval and landslide dam survival time.

In this treatment we are only considering stable landslide dams that erode gradually after they form; this includes dams that stabilize initially or after some degree of catastrophic failure and dam-outburst flood erosion. We acknowledge that many landslides will occur that do not form stable dams, but we do not consider how these non-stable landslides might affect sediment dynamics and the modes by which rivers erode existing landslide dams. These we consider part of the background controls on river incision onto which the effect of river-damming landslides is superimposed. Incorporating the role of outburst floods associated with full or partial failure of landslide dams is an interesting problem that is beyond the scope of the current analysis. We acknowledge that this phenomenon is a mechanism by which large landslide blockages can act to enhance the efficiency of river incision and may act to counteract the negative feedback addressed here.

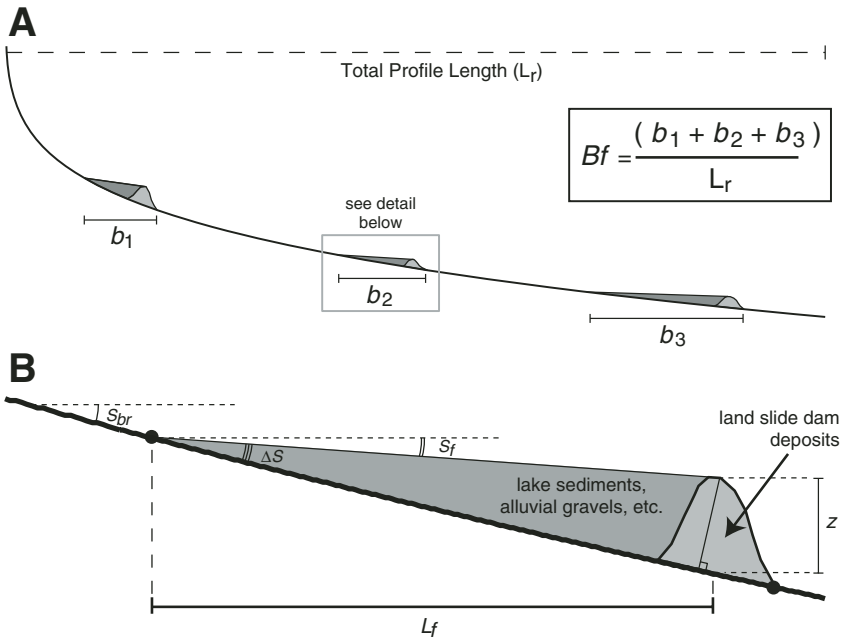

Figure 7. Landslide dams and river profiles. (A) To calculate the landslide burial factor (*Bf*), we sum the individual channel lengths associated with landslide deposits and aggradational wedges behind stable landslide dams. (B) Vertically exaggerated close-up of a landslide dam and the upstream aggradational wedge of sediment associated with it. Note the identification of variables used in Equations 14 through 18. The wedge of sediment behind a landslide dam consists of alluvial gravels and lake sediments. As z_0 decreases, wedge shape is assumed to adjust in a similar manner.

Landslide Dam Occurrence

The first fundamental timescale that influences the average number of landslide dams along a river is the recurrence interval of large landslides that occur randomly along a river and may lead to stable dams (*Ts*). Our model simulates river systems experiencing frequent large landslides, where some subset of landslides that occur lead to stable landslide dams distributed randomly along a length of river. We examine three model scenarios that draw from probability distributions of landslide recurrence intervals, *Ts*, and initial stable dam heights, z_0. In the first scenario, we explore the very simple case in which one stable landslide of fixed height, z_0, occurs at constant recurrence interval *Ts*. In the second scenario, we consider the case in which z_0 and *Ts* vary independently and are normally distributed around fixed mean values. In the third scenario, we investigate the case in which landslide area and resulting stable dam height are derived from a power-law, frequency-magnitude distribution of landslides.

TABLE 1. LANDSLIDE BURIAL FOR CASE STUDIES (FIGURES 4 AND 6)

River name	L_r, channel length of interest (km)	R_r, relief over L_r (m)	Number of active landslide dam sites	*H*, sum of dam heights (m)	Sum of channel lengths buried (km)†	B_r	B_a
Dadu mainstem	90	260	2	100	65	0.72	0.28
Ge Sud Za He	40	760	4	350	30	0.75	0.25
Xiaojin Chuan	40	350	2	160	35	0.88	0.13
Li Qui	180	1800	2	400	70	0.39	0.61

†Burial associated with landslide deposits and upstream wedges of sediment behind dams.

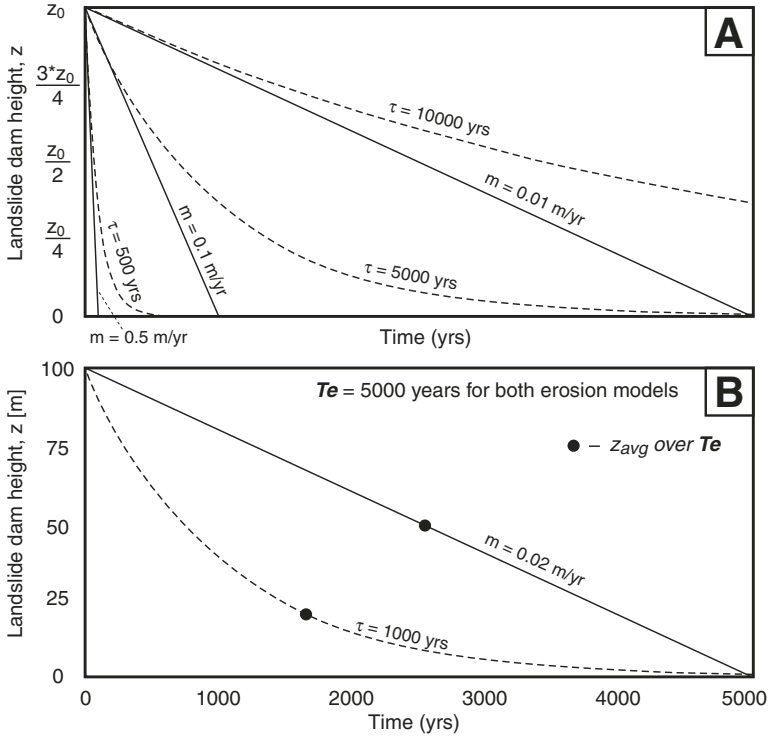

Figure 8. Landslide dam erosion. In our model, stable landslide dams decay in one of two simplified ways—exponentially (dashed lines) or linearly (solid lines). (A) Plots tracking landslide height through time for both erosion scenarios. We give three different curves for each erosion scenario to show the range we use in our model runs. We use values of m and τ to yield *Te* values on the order of 10^1 to 10^5 years. (B) Plot comparing the two erosional scenarios using parameters such that *Te* is the same for both models; in this case, z_0 is 100 m and *Te* is 5000 yr.

In this third model scenario, z_0 and *Ts* are related such that larger landslide dams have much lower recurrence intervals as a consequence of the properties of a power-law distribution. A power-law distribution for medium to large landslides (landslide area $>10^4$ m^2) has been recognized by many authors (e.g., Hovius et al., 1997; Stark and Hovius, 2001; Malamud et al., 2004a). This distribution holds for landslides occurring in space and time throughout a given landscape, and has been documented in diverse landscapes around the world (Hovius et al., 2000; Malamud et al., 2004b). We assume that a subset of all landslides occurring within a landscape will reach the main channel, and furthermore, a subset of these landslides will lead to stable landslide dams. Since this small subset should have the same distribution as the original, we argue that the distribution of stable landslide dams occurring along the length of a river through time is reasonably modeled using a power-law distribution:

$$N_{lsd}(A) = cA^{\beta}, \quad (1)$$

where $N_{lsd}(A)$ is the number of landslide dams that originate from a landslide of area A [m^2], c is the rate of landsliding per year [yr^{-1}], and β is the dimensionless scaling exponent (e.g., Hovius et al., 1997). Our third model scenario generates random landslide events that obey the power-law, frequency-magnitude distribution of Equation 1. As landslides happen, we also use a threshold landslide area (~0.1 km^2, or 10^5 m^2) to set which landslides lead to landslide dams and a conversion factor (20–150 m/km^2) to determine initial landslide dam height from landslide area. Values of this conversion factor are constrained by field examples and published studies of landslide sizes that have led to stable landslide dams (Hewitt, 1998). The resulting distribution of initial landslide dam heights, z_0, scales with the power-law distribution of landslide events that occurred, governed by the scaling parameters β and c, along with the threshold area size and landslide area to landslide dam height conversion factor. We use values of β ranging from 0.7 to 1.4, where higher values of β lead to a steeper frequency magnitude distribution and lower probabilities of occurrence for the largest landslide dams. Coefficient c represents not only the frequency of landslide events, but also the fraction of these events that ultimately form stable landslide dams, such that higher values of c lead to higher probabilities of occurrence for all landslide dams.

Landslide Dam Erosion

The second fundamental timescale that influences the average number and height of landslide dams along a river is the time it takes to incise through landslide deposits, fully breach individual dams, and re-incise through the associated sediment wedge (*Te*). Our model utilizes simple rules of erosion for individual dams to calculate *Te*. Stable landslide dams can act either as masses of tightly packed, large boulders that erode as a whole in essentially the same manner as intact bedrock, or as more loosely packed, immobile boulders that armor the bed, add roughness, dissipate stream energy, and inhibit erosion of the dam during even the highest flows. In addition, landslide deposits may deflect river channels within their valleys and re-incision may incorporate bedrock spurs of the former valley, enhancing the duration of the blockage. We do not attempt to model explicitly these complex processes. Rather we seek only to highlight the fundamental role of the timescale of dam removal.

In our model, stable landslide dams decay either in a linear fashion or exponentially (Fig. 8). Linear erosion proceeds at a specified, constant erosion rate (m). Exponential erosion is based on the premise that incision rate scales with dam height (i.e., downstream knickpoint slope) and is parameterized by a decay timescale (τ). We track landslide height through time, $z(t)$, based on an initial height, z_0, where dz/dt is the rate of change of landslide height.

Exponential erosion incorporates the following equations:

$$dz/dt = -Z/\tau, \quad (2)$$

$$z(t) = z_0 e^{-t/\tau}, \quad (3)$$

$$Te = 5\tau, \quad (4)$$

$$z_{avg} = z_0/5. \quad (5)$$

Linear erosion, by comparison, incorporates:

$$dz/dt = -m, \quad (6)$$

$$z(t) = z_0 - mt, \quad (7)$$

$$Te = z_0/m, \quad (8)$$

$$z_{avg} = z_0/2. \quad (9)$$

In the exponential case, *Te* is 5τ, the time it takes to reduce z_0 to ~1% of its original value (e^{-5} = ~0.01). We adjust values of τ and m to produce *Te* values between tens to ten thousands of years (i.e., faster or slower landslide dam erosion) (Fig. 8A). For each model of erosion, we also calculate a mean landslide dam height over *Te*, denoted z_{avg}. For cases with identical timescales of erosion (*Te*), mean dam height over its life time (z_{avg}) is greatly reduced (by a factor of 40%) in the exponential erosion case owing to the very rapid initial incision (Fig. 8B).

Model Results

Model runs simulate the evolution of landslide dams as they occur and erode along a length of river. The sum of landslide dam heights reflects the total number and size of landslide dams through time (Fig. 9). As erosion parameters are held constant, variability originates from the variability in landslide occurrence (scenarios 1–3). The constant nature of z_0 and *Ts* in scenario 1 leads to a simple, fixed pattern of landslide heights though time, and the approach to long-term average conditions in ~2 ka in this simulation is clear (Fig. 9A). In contrast, the variable nature of landslide distributions used in scenarios 2 and 3 leads to irregular variations in the sum of landslide heights though time. We directly set the variability in scenario 2 by setting the standard deviation of the z_0 and *Ts* distributions (Fig. 9E). Model runs of scenario 2 using small standard deviation are very similar to scenario 1, but as the coefficient of variation increases (ratio of standard deviation to mean), scenario 2 runs deviate from scenario 1, eventually approaching the variability inherent in scenario 3 (Fig. 9F).

The long-term average number of landslide dams that exist at any time (distributed randomly along the length of the river) is set by *Ts* and *Te*. Under the case where *Ts* and *Te* are constants (i.e., scenario 1), the long-term average number of landslide dams is simply the ratio of these timescales (*Te*/*Ts*). Using Equations 4 and 8 for *Te* above, we may write:

$$N_{de} = (5\tau)/Ts, \quad (10)$$

$$N_{dl} = (z_0/m)/Ts, \quad (11)$$

where N_{de} is the long-term average number of landslide dams for the exponential erosion rule, and N_{dl} is the same for the linear erosion rule. Note that the long-term average number of landslide dams using an exponential model of dam erosion (N_{de}) does not depend on the initial height of dams. These expressions for the long-term average number of landslide dams can be combined with any mean property of the distribution to evaluate the integrated effect of all landslides through time. For instance, the product of mean landslide dam height and the long-term average number of dams ($N_d = Te/Ts$) gives the long-term average sum of dam heights, denoted *H*. Using equations for N_d and z_{avg} from Equations 5, 9, 10, and 11, this yields:

$$H_e = (z_0 * \tau/Ts), \quad (12)$$

$$H_l = z_0^2/(2 * m * Ts), \quad (13)$$

where subscripts *e* and *l* refer to exponential and linear erosion rules, respectively. Under scenarios 2 and 3, in which landslide occurrence and initial dam heights are not constant, fixed values of z_0 and *Ts* are replaced by $z_{0\mu}$ and Ts_{μ}, mean values from the distribution of landslides used in the simulation. Analytically derived values for the long-term average sum of landslide heights (dotted line) accurately approximate the numerical results (Fig. 9).

The analytic long-term average describes the long-term mean of summed landslide heights, and should not be considered a static value that numeric simulations asymptotically approach. Model runs that employ linear erosion show more deviation than exponential erosion between analytic long-term average and numerical results, where the analytic long-term average is lower than the long-term mean of summed landslide heights from the simulation under some conditions (Fig. 10). The explanation for this is that exponential erosion is faster than linear erosion in the early stages of landslide dam erosion, so landslide dam heights are reduced to mean values more quickly. This speaks to the significance of large events driving the system. In general, the process of adding landslide material (occurrence) affects the system more because the model adds material very quickly, yet removes it (erosion) slowly; therefore, large landslides will linger in the system longer and have a significant impact on the long-term average sum of heights. For scenario 3, high values of β decrease the occurrence of the largest landslides, and thus lead to a history of summed landslide heights that more closely agrees with analytic long-term average.

Discussion

The long-term average sum of landslide dam heights (*H*) directly implies an average sum of channel lengths buried (i.e., *Bf*) (Fig. 7). Through time, landslide dams erode and their height decreases, changing the length scale of the remaining sediment wedge behind it, assuming that incision back into the sediment wedge is simply limited by incision into the dam blockage. If we consider a length of a large river where drainage area varies minimally along the section of interest such that *Ts*, *Te*, and z_0 are not functions of position along stream, then we can derive simple expressions for the length of upstream fill behind landslide dams. The difference between the bedrock channel slope (S_{br}) and the transport slope of alluvial material filling behind the dam (S_f), denoted Δ*S*, sets the upstream length of fill (L_f) behind a landslide dam from the spill point back (Fig. 7):

$$L_f = z_0/\Delta S. \quad (14)$$

The long-term average length of fill, $(L_f)_{avg}$ and landslide burial factor (*Bf*) follow:

$$(L_f)_{avg} = z_{avg}/(\Delta S), \quad (15)$$

$$Bf = (L_f)_{avg} * (Te/Ts)/L_r, \quad (16)$$

where L_r is the channel length of interest and *Te*/*Ts* is the average number of landslide dams (i.e., N_d in Equations 10 and 11). Combining Equations (15) and (16) gives:

$$Bf = z_{avg} * (Te/Ts)/(\Delta S * L_r) = H/(R_f - S_f * L_r), \quad (17)$$

where *H* is the long-term average sum of heights (i.e., Equations 12 and 13) and R_f is fluvial relief over the river length of interest ($S_{br} * L_r$). Thus, landslide burial *Bf* in the long term is directly proportional to the fraction of fluvial relief represented by drops across landslide knickpoints.

As suggested earlier, we can incorporate *Bf* and the negative feedback effects of large landslides into models of generalized river incision, following Whipple (2004):

$$E = K(1 - B_f) f(qs) A^M S^N, \quad (18)$$

where *E* is erosion rate, *f(qs)* denotes the influence of background sediment flux, *A* is area, *S* is channel slope, exponents *M* and *N* are related to erosion process, and *K* is a coefficient of erosion related to climate and lithology. This simply adds another dimension to *K* from the general form of the stream-power river incision model, such that our new *K*, denoted K_{eff}, is *K*(1-*Bf*). Both steady-state channel slope and transient response time will be functions of K_{eff} (Whipple, 2001; 2004). Higher values of the average sum of dam heights (*H*) produce higher *Bf* (i.e., a stronger landslide effect), and thus lead to slower river incision (i.e., reduced river efficiency), increases in steady-state river gradients, and slower response times to perturbations in tectonic, climatic, or

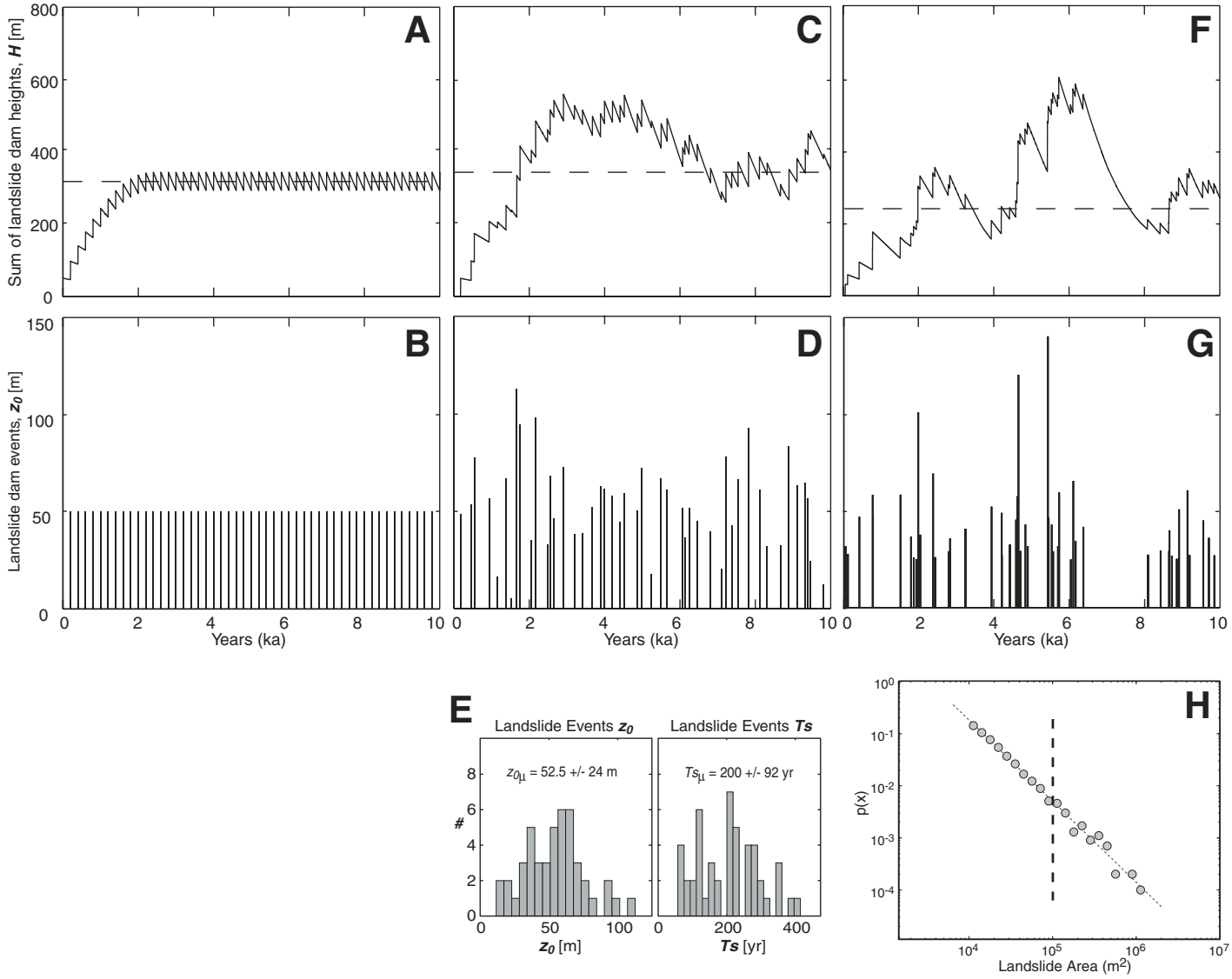

Figure 9. Model runs for each scenario of landslide occurrence using linear erosion for individual landslide dams. Model outputs are plots of the sum of landslide dam height, *H*, through time. In each scenario, the distribution of landslide dams is such that the mean initial stable landslide dam height, z_0, is ~50 m, and the mean recurrence interval of that dam, *Ts*, is ~200 yr. (A) Sum of landslide dam heights through time for a fixed landslide dam height, z_0, occurring at constant recurrence interval, *Ts*. (B) Landslide dam events for (9A) (z_0 = 50 m, *Ts* = 200 yr, *m* = 0.02 m/yr). (C) Sum of landslide dam heights through time, where z_0 and *Ts* vary independently and are normally distributed around fixed mean values. (D) Landslide dam events for (9C) ($z_{0\mu}$ = 52 ± 24 m, Ts_μ = 200 ± 92 yr, *m* = 0.02 m/yr). (E) Distribution of z_0 and *Ts* from (9D). (F) Sum of landslide dam heights through time, where landslide area and resulting stable dam height are derived from a power-law, frequency-magnitude distribution of landslides. (G) Landslide dam events for (9F) ($z_{0\mu}$ = 44 ± 23 m, Ts_μ = 200 ± 279 yr, *m* = 0.02 m/yr). (H) Plot showing the power-law relationship between landslide size and probability, $p(x)$, for the landslide dam events depicted in (9G) (β = 1.5; *c* = 6400 yr^{-1}; landslide area to dam height conversion = 125 m/m^2). Landslides smaller than 0.1 km^2 did not make a stable landslide dam. Dashed lines in (9A), (9C), and (9F) are analytically derived long-term average sum of landslide dam heights for the three scenarios (312 m for scenario 1,337 m for scenario 2, and 242 m for scenario 3) (Equations 12 and 13). Note that these averages are not derived from the entire probability distribution function; they are the averages from the landslide dams that happened randomly in the simulation.

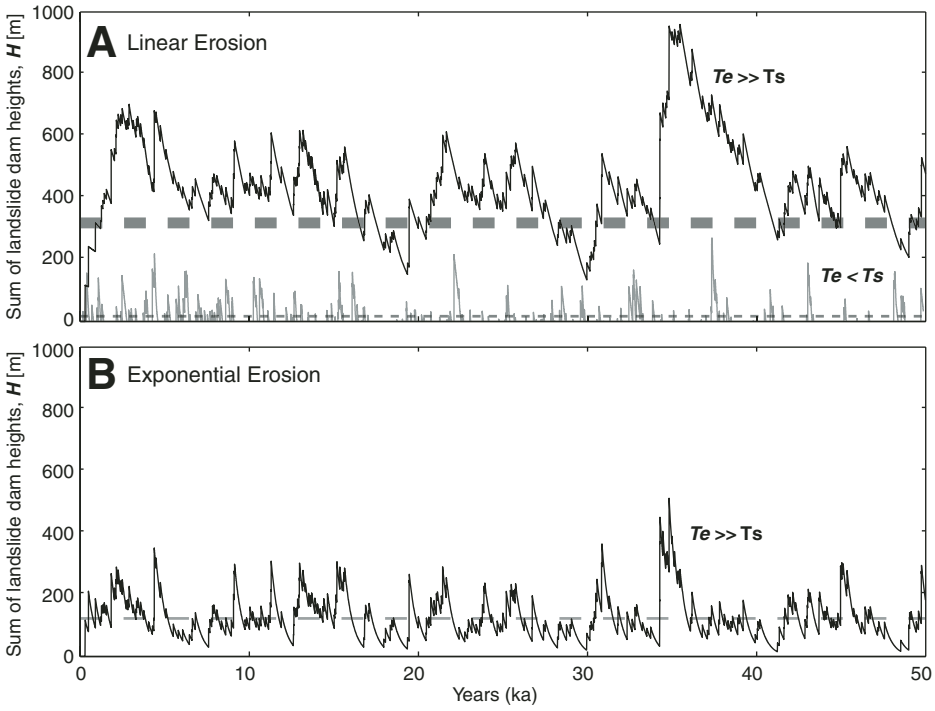

Figure 10. Comparison of model runs that employ linear versus exponential erosion using the same scenario for landslide occurrence (scenario 3) (i.e., Fig. 9F). Each model simulation is 50,000 yr long and the distribution of landslide dams is such that the mean initial stable landslide dam height, z_0, is ~50 m, and the mean recurrence interval of that dam, *Ts*, is ~200 yr. Parameters and thresholds governing the power-law, frequency-size distribution of landslides that occur are the same as shown in Figure 9H. Dashed lines are the analytically derived long-term average sum of landslide dam heights for the two model runs. (A) *Te* >> Ts: Linear erosion (m = 0.02 m/yr). Landslide dam events distribution: $z_{0\mu}$ = 48.8 m ± 34.6 m; Ts_μ = 192.9 ± 200.1 yr; analytical long-term average = ~310 m. *Te* < Ts: Linear erosion (m = 0.5 m/yr). Landslide dam events distribution: $z_{0\mu}$ = 53.2 m ± 36.1 m; Ts_μ = 197.0 ± 202.9 yr; analytical long-term average = ~14 m. (B) *Te* >> Ts: Exponential erosion (τ = 500 yr^{-1}). Landslide dam events distribution: $z_{0\mu}$ = 49.5 m ± 34.3 m; Ts_μ = 198.5 ± 198.8 yr; analytical long-term average = ~127 m. Initially rapid erosion explains the lower long-term average in the case with exponential erosion.

base-level conditions. The high values of *Bf* for select Dadu River channels (Table 1), therefore, suggest slower long-term river incision rates, higher steady-state channel gradients, and more prolonged transient response to regional uplift.

Stable landslide dam size, occurrence, and erosion parameters ultimately dictate the influence of landslides on river incision through their control on N_d and H, and therefore *Bf*. If *Te* << *Ts* (low N_d), landslide dams are eroding more quickly than they are occurring, and the long-term average sum of landslide heights is close to 0, leading to low *Bf* values (Fig. 10). Conversely, if *Te* >> *Ts* (high N_d), the long-term average sum of landslide heights is much greater than zero, and there is a stronger landslide effect (i.e., higher *Bf*). For *Te* >> *Ts*, values of z_0 (or $z_{0\mu}$), *Ts* (or Ts_μ), m, and τ must be such that

$$5 * \tau >> Ts \quad (19)$$

under the exponential erosion model, and

$$z_0/m >> Ts \quad (20)$$

under the linear erosion model. Landscapes prone to a higher density of large landslides, such as those that experience many large earthquakes and/or those experiencing a rapid increase in local relief, will have higher mean values of z_0 and lower mean values of *Ts*, resulting in higher *Te*/*Ts*. Lithology, meanwhile, affects the size of material comprising dam deposits and the erosivity of landslide boulders, both of which can ultimately control z_0. We parameterize the affect of lithology within our model through both z_0 and erosion parameters m and τ; stronger rocks imply longer *Te* (lower m or higher τ), leading to higher *Te*/*Ts*.

Limitations and Guidelines for Further Work

We have intentionally kept our quantitative framework simple enough to highlight the most important aspects of this problem. Many aspects of river profiles must be accounted for to estimate a long-term average *Bf*. Our model considers only the situation in which *Ts*, *Te,* and z_0 are not functions of position along the stream. Along concave-up river profiles, even under steady-state conditions, discharge, channel slope, river and valley widths, hillslope relief, and grain size all vary along stream, and all of these factors might affect the shape and volume of aggradation wedges behind stable landslide dams. Drainage area may affect maximum slide size (local relief), initial landslide dam height (valley width), and the efficiency of landslide dam incision (discharge). In terms of the geometry of the sediment wedge behind landslide dams, drainage area affects the bedrock channel slope, S_{br}, and the transport slope of sediment filling behind the dam, S_f (grain size). There would also need to be rules for overlapping sediment wedges, rules limiting the occurrence of landslides in proximity to recently failed areas, and rules for how landslide distributions link to background incision/erosion rates.

In the short term, landslide dams also greatly impact sediment flux along the river as sediment delivered from upstream is trapped in natural reservoirs, with potentially important consequences for the efficiency of river incision downstream of the dam (e.g., Sklar and Dietrich, 1998; 2004). Once the upstream sediment wedge has aggraded to the spillway height and reestablished the transport slope, however, sediment flux both upstream and downstream of the dam will return to the background rate. This circumstance may prevail for much of the life of a stable landslide dam; our simple model focused on the effect of landslide dam blockages during this phase. Thus we have assumed that away from landslide dams and the associated upstream sediment wedge, the efficiency of bedrock channel incision processes is not perturbed by the presence of upstream landslide dams (i.e., $f(q_s)$ is set by the background sediment flux). A more complete model would account for the transient perturbations associated with the initial aggradation of sediment wedges behind dams.

Future modeling will address these complexities and explore simulations where landslides erode and occur along fully evolving concave-up river profiles. This will allow us to address the direct effects of transient river profile evolution, and how the landslide influence would

interact with transient evolution. We argue, however, that the probabilistic, long-term analysis employed here would hold for such evolving profiles with similar controls and that the same key variables would drive the system and scale of influence. In the end, the controls on *Te* and *Ts*, landslide dam longevity and occurrence, will still dictate the system response.

Our treatment of the effects of landslide dams on river incision excludes the role of outburst floods associated with full or partial failure of landslide dams that occurs before dams stabilize and in cases where no stable dam forms. These floods may act to enhance the efficiency of river incision and potentially counteract the negative feedback we have addressed in this paper. At present, though, it is not clear on theoretical grounds whether the flood enhancement or the burial effect will be more important in the long term. Our field observations tend to indicate that the integrated effect is one of an inhibition of incision, rather than the reverse. A full model of the problem would incorporate the details of dam outburst floods and the complexities of burial on real river profiles. A model like this would probably not be meaningful in the predictive sense, but it could be used to explore the evolution of a river system where we can estimate *Bf* or *Ba* from river profile analysis, satellite image interpretation, and field observations, and where we can constrain the frequency of outburst floods from historic accounts, as we can on the eastern margin on the Tibetan Plateau.

CONCLUSIONS

The illustrative examples from within the Dadu and Yalong river catchments that we have discussed highlight the landslide-dominated character of these rivers and the interaction between incision, landslides, river profiles, and channel morphology typical of rivers throughout the region. As we attempt to understand how river profiles can be used to highlight important aspects of the tectonic and geomorphic evolution of this landscape, mainly as they relate to uplift and transient river adjustment, the effects of large landslides must be addressed. Using simple erosion rules for individual landslide dams and realistic statistical models of how often they occur, we have shown how, and under what circumstances, landslides may significantly impact river incision by regulating where and when channels can and cannot incise. Stable, gradually eroding landslide dams create mixed bedrock-alluvial channels with spatial and temporal variations in incision, ultimately slowing long-term rates of river incision, thereby reducing the total amount of incision occurring over a given length of river per unit time. A stronger landslide effect implies that a higher percentage of channel is buried by landslide-related sediment, leading to reduced river incision efficiency. The longer it takes a river channel to incise into a landslide dam and cut through all landslide-related sediment, the more control these events have on the evolution of the river profile and landscape evolution. This can be the result of slow erosion of dams, a higher frequency of large events, or a denser concentration of landslide dams along a specific river segment.

Our results speak to the dynamic coupling that exists between hillslope erosion by mass movements and river incision. Incision creates the necessary conditions for large landslides to occur (relief and steep hillslopes), but they in turn slow and/or stop river incision by covering the bed for an extended period of time. In such situations, long-term bedrock river incision may proceed through pulses of river incision into bedrock, followed by large landslides, valley filling, and subsequent incision into fill sediments and landslide debris, before river incision into bedrock can continue. The feedback between landslides and river incision is both autogenic (originating from the internal dynamics of long-term river incision) *and* allogenic (driven by transient adjustment to external, outside forcings such as changes in base-level fall, uplift, or climate). Landslides are a fundamental aspect of the transient response to the upstream migration of incision signals, but they also slow it down by reducing river incision efficiency.

The landslide-dominated character of many deep river gorges around the world warrants investigation into how large landslides influence river channels, bedrock river incision, and potentially, landscape evolution. River profiles are often used to make inferences about the tectonic, climatic, base level, and lithologic controls on landscape evolution and the characteristics of transient adjustment to changes in these forcings. However, on spatial and temporal scales relevant to landscape evolution, landslides have effects on channel morphology and river profile form that may be superimposed onto, or directly coupled with, these other controls. By simulating landslide dams occurring and eroding along a length of river and examining controls on the long-term average number and average height of landslide dams, we have begun to quantify the influence of large landslides in actively incising landscapes. Within models of bedrock river incision and landscape evolution, therefore, it is necessary, at a minimum, to include a coefficient of river incision efficiency [$K_{eff} = (1 - Bf)$], which speaks to the spatial and temporal intermittency of incision due to the effects of stable landslide dams.

LIST OF VARIABLES

A	[m^2]	area
β	[-]	dimensionless scaling exponent (power-law distribution of landslides)
Ba	[-]	% river channel not buried, able to incise
Bf	[-]	landslide burial factor (i.e., % river channel buried, not able to incise)
c	[yr^{-1}]	rate of landsliding (power-law distribution of landslides)
dz/dt	[m/yr]	rate of change of landslide height
E	[m/yr]	erosion rate
$f(q_s)$	[-]	influence of sediment flux
H_e	[-]	long-term sum of landslide dam heights for the exponential erosion rule
H_l	[-]	long-term sum of landslide dam heights for the linear erosion rule
K	[-]	coefficient of erosion related to climate and lithology
K_{eff}	[-]	coefficient of erosion incorporating the effects of landslides
L_f	[m]	upstream length of fill behind a landslide dam from the spill-point back
L_r	[m]	channel length of interest
m	[m/yr]	erosion rate for linear erosion of landslide dams
M, N	[-]	exponents related to erosion process
N_{de}	[-]	long-term average number of landslide dams; exponential erosion rule
N_{dl}	[-]	long-term average number of landslide dams; linear erosion rule
N_{lsd}	[-]	number of landslide dams
R_f	[m]	fluvial relief over the river length of interest
S	[-]	channel slope
S_{br}	[-]	bedrock channel slope
S_f	[-]	transport slope of alluvial material filling behind the dam
ΔS	[-]	difference between S_{br} and S_f
τ	[yr]	decay timescale for exponential erosion of landslide dams
Te	[yr]	timescale of erosion for stable landslide dams
Ts	[yr]	timescale of recurrence for stable landslide dams
Ts_μ	[yr]	mean Ts from the distribution of landslides that occur
z	[m]	landslide height
$z(t)$	[m]	landslide height through time
z_{avg}	[m]	mean landslide dam height over Te
z_0	[m]	initial height of the dam
$z_{0\mu}$	[m]	mean z_0 from the distribution of landslides that occur

ACKNOWLEDGMENTS

This work was supported by the National Science Foundation Continental Dynamics program (EAR-0003571), in collaboration with the Chengdu Institute of Geology and Mineral Resources. We wish to thank Joel Johnson, Jamon Frostenson, Tang Fawei, and Miu Guoxia for assistance in the field; Ken Hewitt and Oliver Korup for stimulating discussion; Shannon Mahon for help with preliminary OSL dates; and Darryl Granger, Tom Clifton, Andy Cyr, Marc Caffee, and the Purdue PRIME Lab for help with cosmogenic analysis. We also thank Lewis Owen, Robert Anderson, David Keefer, and an anonymous reviewer for constructive and helpful reviews.

REFERENCES CITED

Allen, C.R., Zhuoli, L., Hong, Q., Xueze, W., Huawei, Z., and Weishi, H., 1991, Field study of a highly active fault zone: The Xianshuihe fault of southwestern China: Geological Society of America Bulletin, v. 103, p. 1178–1199, doi: 10.1130/0016-7606(1991)103<1178:FSOAHA>2.3.CO;2.

Begin, Z.B., Meyer, D.F., and Schumm, S.A., 1980, Knickpoint migration due to base level lowering: American Society of Civil Engineers Journal of the Waterway, Port: Coastal and Ocean Division, v. 106, p. 369–388.

Bookhagen, B., Thiede, R., and Strecker, M., 2005, Late Quaternary intensified monsoon phases control landscape evolution in the northwest Himalaya: Geology, v. 33, no. 2, p. 149–152, doi: 10.1130/G20982.1.

Burbank, D.W., Leland, J., Fielding, E., Anderson, R.S., Brozovic, N., Reid, M.R., and Duncan, C., 1996, Bedrock incision, rock uplift and threshold hillslopes in the northwestern Himalayas: Nature, v. 379, p. 505–510, doi: 10.1038/379505a0.

Burchfiel, B.C., Chen, Zhiliang, Liu, Yuping, and Royden, L.H., 1995, Tectonics of the Longmen Shan and adjacent regions, Central China: International Geology Review, v. 37, no. 8, p. 661–735.

Clark, M.K., House, M.A., Royden, L.H., Whipple, K.X., Burchfiel, B.C., Zhang, X., and Tang, W., 2005, Late Cenozoic uplift of southeastern Tibet: Geology, v. 33, no. 6, p. 525–528, doi: 10.1130/G21265.1.

Clark, M.K., Royden, L.H., Whipple, K.X., Burchfiel, B.C., Zhang, X., and Tang, W., 2006, Use of a regional, relict landscape to measure vertical deformation of the eastern Tibetan Plateau: Journal of Geophysical Research, v. 111, p. F03002, doi: 10.1029/2005JF000294.

Costa, J.E., and Schuster, R.L., 1988, The formation and failure of natural dams: Geological Society of America Bulletin, v. 100, p. 1054–1068, doi: 10.1130/0016-7606(1988)100<1054:TFAFON>2.3.CO;2.

Costa, J.E., and Schuster, R.L., 1991, Documented historical landslide dams from around the world: U.S. Geological Survey Open-File Report 91-239, 486 p.

Crosby, B.T., and Whipple, K.X., 2006, Knickpoint initiation and distribution within fluvial networks: 236 waterfalls in the Waipaoa River, North Island, New Zealand: Geomorphology, v. 82, p. 16–38.

Dai, F.C., Lee, C.F., Deng, J.H., and Tham, L.G., 2005, The 1786 earthquake-triggered landslide dam and subsequent dam-break flood on the Dadu River, southwestern China: Geomorphology, v. 65, p. 205–221, doi: 10.1016/j.geomorph.2004.08.011.

Densmore, A., Ellis, M., and Anderson, R., 1998, Landsliding and the evolution of normal-fault-bounded mountains: Journal of Geophysical Research, v. 103, p. 15203–15219, doi: 10.1029/98JB00510.

Gasparini, N.M., 2003, Long-term average and transient morphologies of river networks: Discriminating among fluvial erosion models [Ph.D. thesis]: Cambridge, Massachusetts Institute of Technology.

Gasparini, N.M., Bras, R.L., and Whipple, K.X., 2006, Numerical modeling of non-steady-state river profile evolution using a sediment-flux-dependent incision model, *in* Willett, S.D., Hovius, N., Brandon, M.T., and Fisher, D., eds., Tectonics, climate, and landscape evolution: Geological Society of America Special Paper 398, p. 127–142.

Hasbargen, L., and Paola, C., 2000, Landscape instability in an experimental drainage basin: Geology, v. 28, no. 12, p. 1067–1070, doi: 10.1130/0091-7613(2000)28<1067:LIIAED>2.0.CO;2.

Hejun, C., Hanchao, L., Zhuoyuan, Z., and Zhiwen, X., 2000, The distribution, causes and effects of damming landslides in China: Journal of the Chengdu University of Technology, v. 27, no. 3, p. 302–307.

Hewitt, K., 1998, Catastrophic landslides and their effects on the Upper Indus streams, Karakorum Himalaya, northern Pakistan: Geomorphology, v. 26, p. 47–80, doi: 10.1016/S0169-555X(98)00051-8.

Hewitt, K., 2006, Disturbance regime landscapes: Mountain drainage systems interrupted by large rockslides: Progress in Physical Geography, v. 30, no. 3, p. 365–393, doi: 10.1191/0309133306pp486ra.

Hovius, N., Stark, C.P., and Allen, P.A., 1997, Sediment flux from a mountain belt derived by landslide mapping: Geology, v. 25, p. 231–234, doi: 10.1130/0091-7613(1997)025<0231:SFFAMB>2.3.CO;2.

Hovius, N., Stark, C.P., Chu, H.-T., and Lin, J.C., 2000, Supply and removal of sediment in a landslide-dominated mountain belt: Central Range, Taiwan: The Journal of Geology, v. 108, no. 1, p. 73–89, doi: 10.1086/314387.

Howard, A.D., 1994, A detachment-limited model of drainage basin evolution: Water Resources Research, v. 30, p. 2261–2285, doi: 10.1029/94WR00757.

Keefer, D.K., 1994, The importance of earthquake-induced landslides to long-term slope erosion and slope-failure hazards in seismically active regions: Geomorphology, v. 10, p. 265–284, doi: 10.1016/0169-555X(94)90021-3.

Kirby, E., Reiners, P.W., Krol, M.A., Whipple, K.X., Hodges, K.V., Farley, K.A., Tang, W., and Chen, Z., 2002, Late Cenozoic evolution of the eastern margin of the Tibetan Plateau: Inferences from 40Ar/39Ar and (U-Th)/He thermochronology: Tectonics, v. 21, no. 1, p. 1001, doi: 10.1029/2000TC001246, doi: 10.1029/2000TC001246.

Kirby, E., Whipple, K.X., Tang, W., and Chen, Z., 2003, Distribution of active rock uplift along the eastern margin of the Tibetan Plateau: Inferences from bedrock channel longitudinal profiles: Journal of Geophysical Research, v. 108, B4, p. 2217, doi: 10.1029/2001JB000861.

Kobor, J.S., and Roering, J.J., 2004, Systematic variation of bedrock channel gradients in the central Oregon Coast Range: Implications for rock uplift and shallow landsliding: Geomorphology, v. 62, p. 239–256, doi: 10.1016/j.geomorph.2004.02.013.

Korup, O., 2002, Recent research on landslide dams—A literature review with special attention to New Zealand: Progress in Physical Geography, v. 26, no. 2, p. 206–235, doi: 10.1191/0309133302pp333ra.

Korup, O., 2005, Geomorphic imprint of landslides on alpine river systems, southwest New Zealand: Earth Surface Processes and Landforms, v. 30, no. 7, p. 783–800, doi: 10.1002/esp.1171.

Korup, O., 2006, Rock-slope failure and the river long profile: Geology, v. 34, no. 1, p. 45–48, doi: 10.1130/G21959.1.

Korup, O., Strom, A., and Weidinger, J., 2006, Fluvial response to large rock-slope failures: Examples from the Himalayas, the Tien shan, and the southern Alps in New Zealand: Geomorphology, v. 78, no. 1–2, p. 3–21.

Lague, D., Crave, A., and Davy, P., 2003, Laboratory experiments simulating the geomorphic response to tectonic uplift: Journal of Geophysical Research, v. 108, B1, p. 2008, doi: 10.1029/2002JB001785.

Malamud, B.D., Turcotte, D.L., Guzzetti, F., and Reichenbach, P., 2004a, Landslide inventories and their statistical properties: Earth Surface Processes and Landforms, v. 29, no. 6, p. 687–711, doi: 10.1002/esp.1064.

Malamud, B.D., Turcotte, D.L., Guzzetti, F., and Reichenbach, P., 2004b, Landslides, earthquakes and erosion: Earth and Planetary Science Letters, v. 229, no. 1-2, p. 45–59, doi: 10.1016/j.epsl.2004.10.018.

Pratt, B., Burbank, D., Heimsath, A., and Ojha, T., 2002, Impulsive alluviation during early Holocene strengthened monsoons, central Nepal Himalaya: Geology, v. 30, no. 10, p. 911–914, doi: 10.1130/0091-7613(2002)030<0911:IADEHS>2.0.CO;2.

Roger, F., Malavieille, J., Leloup, H., Calassou, S., and Xu, Z., 2004, Timing of granite emplacement and cooling in the Songpan–Garze Fold Belt (eastern Tibetan Plateau) with tectonic implications: Journal of Asian Earth Sciences, v. 22, p. 465–481, doi: 10.1016/S1367-9120(03)00089-0.

Schmidt, K.M., and Montgomery, D.R., 1995, Limits to relief: Science, v. 270, p. 617–620, doi: 10.1126/science.270.5236.617.

Sklar, L., and Dietrich, W.E., 1998, River longitudinal profiles and bedrock incision models: Stream power and the influence of sediment supply, *in* Tinkler, K.J., and Wohl, E.E., eds., Rivers over rock: Fluvial processes in bedrock channels: Geophysical Monograph Series, v. 107, p. 237–260.

Sklar, L., and Dietrich, W.E., 2001, Sediment supply, grain size and rock strength controls on rates of river incision into bedrock: Geology, v. 29, no. 12, p. 1087–1090, doi: 10.1130/0091-7613(2001)029<1087:SARSCO>2.0.CO;2.

Sklar, L., and Dietrich, W.E., 2004, A mechanistic model for river incision into bedrock by saltating bed load: Water Resources Research, v. 40, doi: 10.1029/2003WR002496.

Sklar, L., and Dietrich, W.E., 2006, The role of sediment in controlling steady-state bedrock channel slope: Implications of the saltation-abrasion incision model: Geomorphology, v. 82, p. 58–83.

Stark, C., and Hovius, N., 2001, The characterization of landslide size distributions: Geophysical Research Letters, v. 28, p. 1091–1094, doi: 10.1029/2000GL008527.

Tianchi, L., 1990, Landslide management in the mountain areas of China: ICIMOD Occasional Paper No. 15, Kathmandu, Nepal.

Trauth, M.H., Bookhagen, B., Marwan, N., and Strecker, M.R., 2003, Multiple landslide clusters record Quaternary climate changes in the NW Argentine Andes: Palaeogeography, Palaeoclimatology, Palaeoecology, v. 194, p. 109–121, doi: 10.1016/S0031-0182(03)00273-6.

Tucker, G.E., Catani, F., Rinaldo, A., and Bras, R.L., 2001, Statistical analysis of drainage density from digital terrain data: Geomorphology, v. 36, p. 187–202, doi: 10.1016/S0169-555X(00)00056-8.

U.S. Geological Survey, 1993, Digital elevation models–Data user guide 5: Reston, Virginia, U.S. Geological Survey, p. 48.

Whipple, K.X., 2001, Fluvial landscape response time: How plausible is steady-state denudation?: American Journal of Science, v. 301, p. 313–325, doi: 10.2475/ajs.301.4-5.313.

Whipple, K.X., 2004, Bedrock rivers and the geomorphology of active orogens: Annual Review of Earth and Planetary Sciences, v. 32, p. 151–185, doi: 10.1146/annurev.earth.32.101802.120356.

Whipple, K.X., and Tucker, G.E., 2002, Implications of sediment-flux dependent river incision models for landscape evolution: Journal of Geophysical Research, v. 107, no. B2, doi: 10.1029/2000JB000044.

Willgoose, G., Bras, R.L., and Rodriguez-Iturbe, I., 1991, A coupled channel network growth and hillslope evolution model, 1. Theory: Water Resources Research, v. 27, p. 1671–1684, doi: 10.1029/91WR00935.

Wobus, C.W., Whipple, K.X., Kirby, E., Snyder, N.P., Johnson, J., Spyropolou, K., Crosby, B.T., and Sheehan, D., 2006, Tectonics from topography: Procedures, promise, and pitfalls, *in* Willett, S.D., Hovius, N., Brandon, M.T., and Fisher, D., eds., Tectonics, climate, and landscape evolution: Geological Society of America Special Paper 398, p. 55–74.

Manuscript Received 4 November 2006
Revised Manuscript Received 30 May 2007
Manuscript Accepted 7 June 2007

Printed in the USA